Available online at www.sciencedirect.com
SCIENCE DIRECT
Carbohydrate Polymers 62 (2005) 369–378
Carbohydrate Polymers
www.elsevier.com/locate/carbpol

Chemical force microscopy of cellulosic fibers

Juan C. Bastidas [a], Richard Venditti [a], Joel Pawlak [a], Richard Gilbert [a], Stefan Zauscher [b], John F. Kadla [c,*]

[a] Department of Pulp and Paper Science Raleigh, North Carolina State University, NC, USA
[b] Department of Mechanical Engineering and Materials Science, Duke University, Durham, NC, USA
[c] Biomaterials Chemistry, Faculty of Forestry, University of British Columbia, 4034-2424 Main Mall, Vancouver, BC, Canada V6T 1Z4

Received 17 June 2005; accepted 12 August 2005
Available online 21 October 2005

Abstract

Atomic force microscopy with chemically modified cantilever tips (chemical force microscopy) was used to study the pull-off forces (adhesion forces) on cellulose model surfaces and bleached softwood kraft pulp fibers in aqueous media. It was found that for the –COOH terminated tips, the adhesion forces are dependent on pH, whereas for the $–CH_3$ and –OH terminated tips adhesion is not strongly affected by pH. Comparison between the cellulose model surfaces and cellulosic fibers under our experimental conditions reveal that surface roughness does not affect adhesion strongly. X-ray photoelectron spectroscopy (XPS) and Fourier Transformed Infrared (FTIR) spectroscopy reveal that both substrate surfaces have homogeneous chemical composition. The results show that chemical force microscopy can be used for the chemical characterization of cellulose surfaces at a nano-level.

Keywords: Atomic force microscopy (AFM); Chemical force microscopy (CFM); SAMS; XPS; Cellulose fibers; Cellulose film; Pull-off forces; Adhesion forces

1. Introduction

Understanding the surface chemical and morphological properties of natural fibers is critical for their efficient utilization in various bioproducts. As a composite biomaterial, natural fibers have compositional and morphological variation in the surface and bulk domains, thereby adding complexity to their accurate characterization. Few analytical techniques are able to characterize the surface composition of fibers with sensitivity to the local topographical and compositional variations (Hanley & Gray, 1995).

Atomic force microscopy (AFM) is a unique technique for the study of material surfaces as it provides not only topographic profiles of the surface but also chemical information at the nanoscale based on the interaction between the scanning probe tip and the surface (Duwez & Nysten, 2001). Chemical force microscopy (CFM) is a variation of AFM in which the probe is modified with specific functional groups (e.g. polar or non-polar) and the recorded interactions between the probe and surface are used to explore the chemical composition of the surface (Noy, Vezenov & Lieber, 1997).

The ability to resolve surface features with nanometer spatial resolution have made the AFM a powerful tool to examine the ultrastructure of natural materials, such as cellulose (Hanley & Gray, 1995) and individual wood pulp fibers and paper surfaces (Gray, Furuta, Pang & Nilsson, 1991).

During the chemical pulping processing of wood, lignin and hemicelluloses are largely removed from the fiber, leaving cellulose as the major component. AFM without tip modification has been used to study changes in the surface of pulp fibers during pulping and delignification processes (Wistara, Zhang & Young, 1999; Simola-Gustafsson, Hortling & Peltonen, 2001; Pereira, Chernoff, Claudio-Da-Silva & Demuner, 2001; Boras & Gatenholm, 1999). Intermittent contact imaging (Tapping® mode imaging, Digital Instruments), can distinguish variations in surface composition due to differences in the local visco-elastic properties within a sample (Babcock & Prater, 1995). Intermittent contact imaging revealed lignin-rich granular and cellulose-rich fibrillar surface structures in different extents after delignification processes, i.e. pulping and bleaching. This interpretation was supported by conventional lignin determination measurements (Kappa Number) and X-ray photoelectron spectroscopy (XPS).

* Corresponding author. Tel.: +1 6048275254, fax: +1 6048229104.
E-mail address: john.kadla@ubc.ca (J.F. Kadla).

0144-8617/$ - see front matter © 2005 Elsevier Ltd. All rights reserved.
doi:10.1016/j.carbpol.2005.08.058

Specific tip–surface interactions can be studied by chemical modification of the tip and/or the surface (Duwez & Nysten, 2001; Noy et al., 1997; Senden, 2001; Prater, Maivald, Kjoller & Heaton, 1998; Schönherr, Hruska & Vancso, 2000; Ton-That, Teare & Bradley, 2000; Duwez, Poleunis, Bertrand & Nysten, 2001; Cappella & Dietler, 1999; Schonherr, Hruska & Vancso, 1998).

Studies that involve the use of force measurements between the probe and natural fiber surfaces have been made (Furuta & Gray, 1998; Pang & Gray, 1998; Irvine, Aston & Berg, 1999). For example, Gray and coworkers (Furuta & Gray, 1998) measured the force interactions between non-modified silicon nitride AFM tips and bleached softwood kraft pulp fibers in aqueous media as a function of ionic strength. They found that long-range repulsive interactions exist in domains of the cell wall where microfibrils extended away from the surface. This long-range repulsion decreases with increasing salt concentration and is believed to arise from fibril–fibril and fibril–surface electrostatic and steric interactions.

To date, force measurements on cellulosic fibers were more qualitative, as the probe chemistry was not well defined. In this work, our objective was to determine the utility of CFM as an analytical tool to characterize the chemical composition and functionality of pulp fiber surfaces. Specifically, the influence of pH on the pull off forces on cellulose surfaces was measured for probe tips with hydroxyl, acidic and methyl terminated functional groups.

2. Materials and methods

2.1. Materials

Commercial softwood bleached kraft pulp was chosen as an appropriate industrial material for the initial evaluation of chemical force microscopy on a natural cellulosic fiber. The pulp was fractionated in a Bauer McNett Classifier and the fraction retained on mesh 12 (screen size opening of 1.68 mm) was used for AFM analysis. A characterization of this fraction is shown in Table 1.

Table 1
Characterization of bleached softwood Kraft fibers

Mean fiber length[a]	
Length weighted	3.47 mm
Fines, length weighted	0.03%
Chemical analysis	
α-cellulose[b]	88.8%
Sugar analysis[c]	
Glucose	81.54%
Xylose	9.40%
Mannose	6.54%
Arabinose	0.37%
Galactose	0.22%
Lignin-soluble	0
-insoluble	0.24%

[a] Fiber length determined by FQA (Optest Equipment Inc.).
[b] As per Yokoyama et al. (2002).
[c] As per Mansfield et al. (1997).

2.2. Pulp fiber characterization

Fiber length was determined using a fiber quality analyzer (FQA, Op Test Equipment, Inc.). Cellulose and hemicellulose contents were determined using the method proposed by Yokoyama et al. (Yokoyama, Kadla & Chang, 2002). Specifically, 300 mg of dry fiber was weighed into a 100 mL beaker and mixed with 20.0 mL of 17.5 (NaOH (Fisher Scientific) using a glass rod. The fiber and NaOH was reacted for 30 min, at which point 20 mL of deionized water was added, the mixture was stirred and allowed to further react for 30 min. The fiber suspension was filtered using a coarse glass filter, washed thoroughly with deionized water and soaked in 1.0 M acetic acid (Fischer Scientific) for 5 min. The neutralized α-cellulose was washed thoroughly with deionized water, oven-dried at 105 °C and weighed. The material removed during the alkali extraction represents the hemicellulose component.

Sugars were determined using the method described by Mansfield et al. (Mansfield, De Jong & Saddler, 1997). In this method, pulp fibers are degraded from their macromolecular structure to individual monomeric constituents by acid hydrolysis and then quantified by High Performance Liquid Chromatography (HPLC).

For AFM measurements the fibers were mounted on glass surfaces according to the method described by Futura and Gray (Furuta & Gray, 1998). In this procedure, the fibers were suspended in water and a drop was placed on top of a clean glass cover slide (which has been previously immersed in 70 (sulfuric acid (Fisher Scientific) and repeatedly washed with deionized water). The water was allowed to evaporate gently overnight under ambient conditions. Upon the evaporation of the water the fiber adhered to the glass surface and remained adhered to the glass even after subsequent immersion in water.

2.3. Cellulose model surfaces

Cellulose model surfaces were prepared according to the procedure described by Zauscher (Zauscher & Klingenberg, 2001). A film of regenerated cellulose (Spectra/Por 1 membrane, molecular weight cutoff 6–8 kDa (Spectrum Lab)) was extracted twice with dichloromethane (Acros Organics) and acetone (Fischer Scientific) to remove glycerine and other organic surface contaminants. After drying in an oven at 105 °C and cooling in a desiccator, the cellulose films were attached to a glass slide (Fisherbrand Superfrost® microscope slides) using a very thin film of an epoxy resin (Stix-On Contact™, Power Poxy Adhesives), and allowed to cure for 24 h.

2.4. Tip chemical modification and model surface preparation

Triangular shaped silicon nitride cantilevers with silicon nitride tips (Digital Instruments (DI), Santa Barbara, CA, part No. DNP-S20) were coated with 10 nm Cr and 270 nm Au in a thermal, high vacuum evaporator (Veeco Instruments). Flat Au substrates were prepared by the same procedure applying

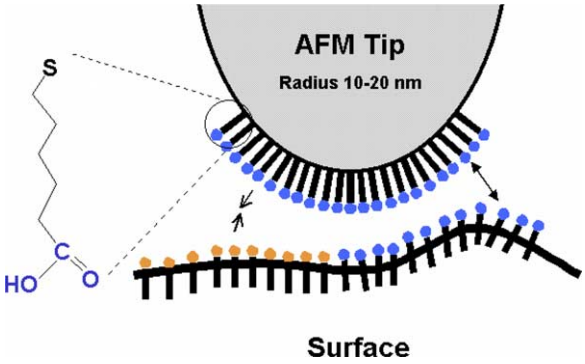

Fig. 1. CFM principle: chemical tip modification with self assemble monolayers (SAMs).

30 nm Cr and 400 nm Au to 1 cm × 1 cm glass slides (Fisherbrand Superfrost® microscope slides) (Duwez, Poleunis, Bertrand, Nysten, 2001). For chemical modification 1-octadecanethiol $CH_3(CH_2)_{17}SH$ (Aldrich), 11-mercapto-1-undecanol $OH(CH_2)_{11}SH$ (Aldrich), 11-mercaptoundecanoic acid $HOOC(CH_2)_{10}SH$ (Aldrich) and HPLC grade alcohol (Fischer Scientific) were used as received.

Prior to their use, the gold-coated tips and gold substrates were cleaned using a short wave 254 nm UV lamp (Spectroline® model EF-140C, Spectronics Corporation) for 1 h to ensure that all organic material was removed (Ron & Rubinstein, 1994). Immediately after the cleaning step, the gold-coated tips and substrates were immersed in reagent alcohol for 30 min. Chemical modification was performed by immersing the gold-coated tips and substrates into a 1 mM $CH_3(CH_2)_{17}SH$, $OH(CH_2)_{11}SH$ or $HOOC(CH_2)_{10}SH$ alcoholic solution for 2 h at room temperature. Finally, the modified tips and substrates were rinsed with *n*-heptane (Aldrich) and alcohol, and gently dried in an Argon stream. The resulting self assembled monolayer surfaces (SAMS) were then store under nitrogen prior to use. Fig. 1 shows a schematic representation of a modified tip.

2.5. AFM measurements

AFM measurements were performed with a Dimension 3000 microscope (Digital Instruments (DI), Santa Barbara, CA) using a fluid imaging cell. The measurements were carried out in buffered aqueous solutions. Three solutions of phosphate salts were initially prepared at 0.01 M concentration: Na_3PO_4 (Aldrich), Na_2HPO_4 (Aldrich) and NaH_2PO_4 (Fisher Scientific). Buffer solutions covering a pH range from 2 to 10 were prepared with mixtures of the solutions; low pH solutions required adjustment with diluted HCl (Fisher Scientific) (Schönherr, Hruska & Vansco 2000).

For the chemically modified gold surfaces, AFM Measurements were performed after a solution/surface contact period of approximately 1 h. For cellulose membranes and fiber surfaces, AFM measurements were performed after a solution/surface equilibration period of 3 h. Force vs. cantilever displacement curves were used to obtain adhesive interaction data between the tip and sample. The pull-off force (adhesion) was defined as the maximum force required to retract the probe from the surface. For every experiment, the average value of pull-off forces was determined from 50 force–distance curves (Duwez, Poleunis, Bertrand, Nysten, 2001), obtained from 'force–volume®' imaging. In this way, the spatial distribution of the interaction force between the tip and the surface could be obtained. These curves were obtained for at least two fibers and at least two areas of each fiber. RMS roughness data were obtained analyzing topography images with the software included in the AFM equipment, using 5 μm scan area as a total area for the measurements.

2.6. Surface analysis by XPS and FTIR

X-ray photoelectron spectra of cellulose film and pulp fiber surface (handsheets) were obtained with a Riber LAS 3000 with MAC Analyzer XPS analyzer equipped with Mg Kα source (1254 eV), operated at 12 kV, 14 mA and charge compensation with an electron flood gun. The detector position was at an angle of 20° in relation with the sample surface. The analyzed area was ≈5 mm^2. Prior to each measurement, samples were mounted and left overnight in the equipment chamber to equilibrate with the surrounding environment, a step required for hygroscopic samples such as paper (Johansson, Campbell, Koljonen & Stenius, 1999). At least three different locations on each sample were analyzed. A fitting program—Peakfit 4.1 (Systat Software Inc.) was used to deconvolute the C1s signal into Gaussian components having equal full width at half maximum (FWHM) values, and binding energy ranges relative to the C–C position of 1.55–1.69 eV for C–O and 3.13–3.31 eV for O–C–O or C=O groups (Zauscher, 2000a; Johansson, 2002).

FT-IR spectra of the surface samples were obtained using a Nexus spectrophotometer (Nexus 670 Thermonicolet) and the Omnisampler analyzer for Attenuated Total Reflection (ATR). The specimens were air dried before taking the spectra. Due to water and carbon dioxide in the surrounding air, the automatic atmospheric suppression capability of the equipment software was used.

3. Results and discussion

3.1. Interaction between modified tips and model surfaces

The quality of the chemically modified tips was assessed by measuring the adhesive interaction on model surfaces (Fig. 2). The average values follow the trends and order of magnitude described by Noy, Vezenor & Lieber (1997). The absolute value of the pull-off force depends on the individual probe tip radius and cantilever spring constant, which vary from probe to probe. Thus, it is only reasonable to directly compare the pull-off forces for a single probe (Fig. 2(a)), but results from different probes can only be compared on a 'order of magnitude' basis (Fig. 2(a vs. b)). This method to validate the quality of tip modification is used routinely, since common spectroscopic techniques are unable to characterize the chemical composition of cantilever tips on the nanometer scale (Duwez, Poleunis, Bertrand & Nysten, 2001).

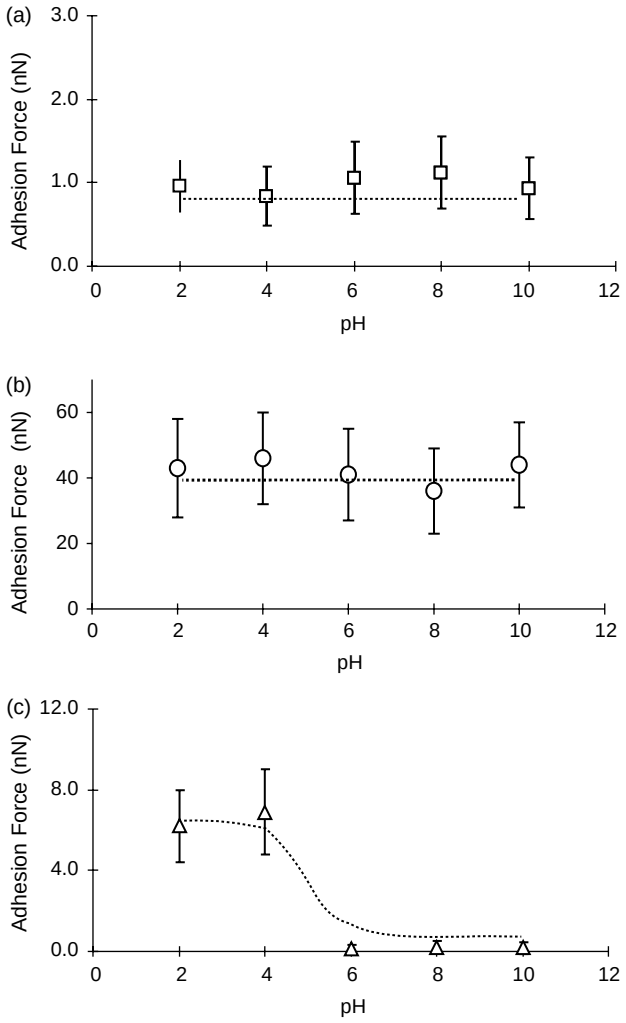

Fig. 2. Adhesive forces for the interaction between modified tips and model surfaces: (a) OH tip/OH surface; (b) CH_3 tip/CH CH_3 surface; (c) COOH tip/COOH surface.

Two of the tip/surface pairs, CH_3/CH_3 and OH/OH, show a relative constant force over the pH range studied, and can be explained by the acid–base behavior for these probes-surfaces. The end groups (CH_3 and OH) do not dissociate in the pH range studied, and adhesion thus largely depends on Van der Waals forces and hydrogen bonding which remain basically constant. However, the adhesion force magnitude is different for the two systems, $\approx$1 nN for the OH/OH system and $\approx$40 nN for CH_3/CH_3 system. This difference can be explained by a solvent exclusion effect: water does not wet the hydrophobic methyl-terminated surfaces, and a large pull-off force is thus needed to break the tip-sample contact (Sinniah, Steel, Miller & Reutt-Robey, 1996).

Distinct from the other two, the COOH/COOH tip/surface system shows a titration curve-like behavior. At pH values (4.0, adhesion forces are large ($\sim$7.0 nN) and decrease with increasing pH, leveling near to zero for pH(7.0 (Fig. 2(c)). The pH dependent behavior can be explained considering the interactions between the COOH groups on the tip and the substrate (Noy, Vezenov & Lieber, 1997; Smith, Wallwork, Zhang, Kirkham, Robinson & Marsh 2000; He, Huang, Zhang, Li, Li, & Liu 2000). At low pH levels (pH(4) the COOH groups are protonated and not charged, and the adhesion force likely originates from van der Waals forces and hydrogen bonding between tip and substrate. As the pH increases, the acidic group gradually becomes deprotonated and the negative charge is delocalized throughout the carboxylate group, which decreases the amount of hydrogen bonding and the adhesion force. Simultaneously, the electrostatic repulsion between the charged COO^- groups increases leading to a further decrease in the adhesion force. Above pH 7.0, (99%) of the acid groups are deprotonated, and causing strong electrostatic repulsion.

To obtain information about the magnitude of forces between surfaces of different polarity, force measurements at different pH values were performed for various combinations of tip(surface functionality (Fig. 3). For the pair CH_3/OH, almost a constant adhesion force value for the range of pH from 2 to 10 was seen (Fig. 3(a)), and is consistent with the absence of a protonation–deprotonation process (Duwez, Poleunis, Bertrand & Nysten, 2001; Sinniah, Steel, Miller & Reutt-Robey 1996; Papastavrou &

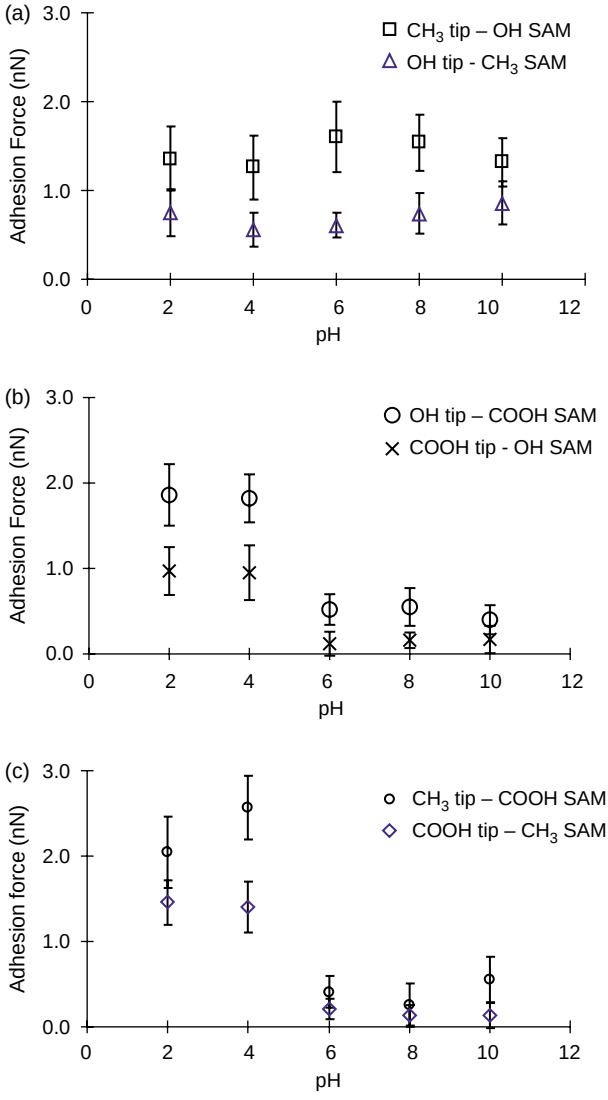

Fig. 3. Adhesive forces for the interaction between modified tips and model surfaces: (a) OH/CH_3 pair; (b) OH/COOH pair; (c) CH_3/COOH pair.

Akari, 2000). It has been suggested that the presence of a hydrophobic surface in water leads to a domination of hydrophobic forces over other interaction forces (Papastavrou & Akari, 2000), and a theoretical explanation has been suggested based on the surface tension component approach (Vezenov, Zhuk, Whitesides & Lieber, 2002; Freitas & Sharma, 2001).

For the COOH functionalized tip on both the polar OH and non-polar CH_3 functionalized surfaces, at pH(5 the pull-off force are small (Fig. 3(b,c)). Under these conditions the COOH group is ionized, producing a negative charge on the tip surface and a predominately electrostatic repulsive interaction, with the presence of almost no pull-off forces. At pH values less than 4, however, pull-off forces exist and can be explained by the interaction between unprotonated COOH and surface groups. For the OH tip, hydrogen bonding interactions occur with the COOH surface and a similar pH effect is observed. For the CH_3 tip and the COOH surface, the non polar monolayer cannot participate in acid–base interactions. However, Fig. 3(c) suggests a degree of solvent participation in the enhancement of adhesion force when protonated COOH groups are present. The same phenomenon is observed for the hydrophobic CH_3 surface and the non-charged polar tip (COOH) in the water medium. This apparent abnormal behavior has been reported by other researchers studying hydrophobic–hydrophilic interactions in aqueous media, where the surface tension component approach is used to explain it, especially at low pH (Duwez, Poleunis, Bertrand & Nysten, 2001; Sinniah, Steel, Miller & Reutt Robey, 1996; Papastavrou & Akari, 2000; Vezenov, Zhuk, Whitesides & Lieber, 2002; Freitas & Sharma, 2001).

3.2. Interaction of modified tips with cellulose films and fibers

Adhesion force values for the interaction of modified tips and cellulose surfaces are shown in Figs. 4–6. In all cases, the interaction of the protonated COOH tips (pH 4) with cellulosic surfaces is greater than the interaction with ionized COO^- tips (pH 6), showing a similar trend as the SAM model surfaces (Fig. 3(b,c)).

As with the model surfaces the extracted and non-extracted pulp fibers exhibit pH dependent pull-off forces. The force values measured between the OH tip and the fiber surfaces are similar to the forces observed between the OH model surface and OH tip, indicating a similar surface composition. In a fully bleached fiber, the main component of the surface will be cellulose, having several OH groups per repeat unit. The adhesion forces between the OH(OH groups in aqueous media are low as the media affects the interaction between the phases, minimizing van del Waals interactions (Papastavrou & Akari, 2000).

For the COOH tip larger pull-off forces are observed in the pH region from 2.0 to 4.0 when compared to forces in the pH region of 6 to 10. This is qualitatively the same behavior as the COOH/OH and COOH/CH_3 tip(model surface pairs described in Fig. 3, wherein ionization of the carboxylic groups lead to a near zero pull-off force. Despite significant differences in topographical features between pulp fibers and the model surfaces (discussed below) the surface chemical interactions are quite similar. For the hydrophobic CH_3 tip the adhesion force measured on the fiber surface is almost zero. This is quite different from the results obtained between the model surfaces (CH_3/OH pair), where small but consistent adhesion forces were observed. This may be due to accessibility of the surface

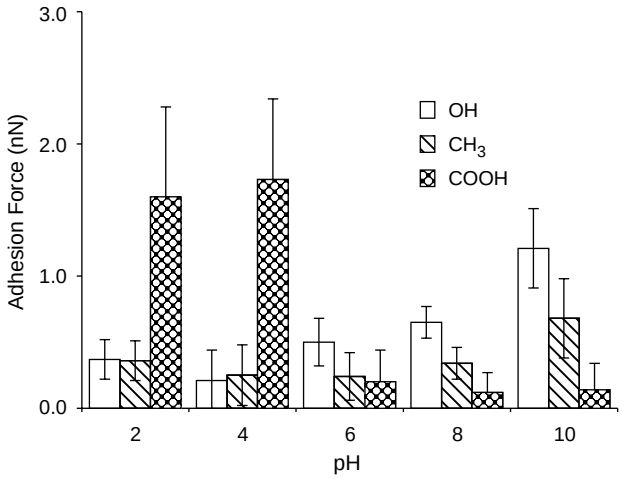

Fig. 5. Interactions between modified tips and cellulose fibers: pull-off force values at several pH using functionalized tips with OH, COOH and CH_3 end groups.

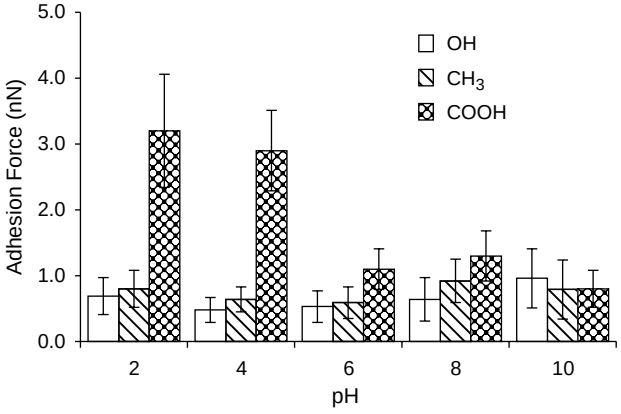

Fig. 4. Interactions between modified tips and cellulose films: pull off force values at several pH using functionalized tips with OH, COOH and CH_3 end groups.

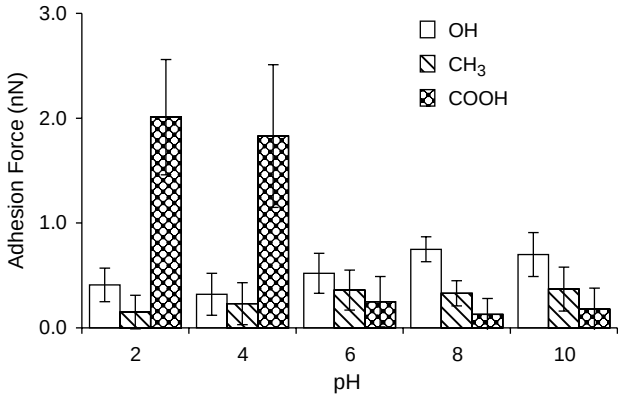

Fig. 6. Interactions between modified tips and extracted cellulose fibers: pull-off force values at several pH using functionalized tips with OH, COOH and CH_3 end groups.

Table 2
RMS roughness (nm) values for SAMS, cellulose film and cellulose fiber surfaces

TIP pH	SAMS			Cellulose film			Cellulose fiber			Extracted cellulose fiber		
	OH	CH_3	COOH	OH	CH_3	COOH	OH	CH_3	COOH	OH	CH_3	COOH
2.0	1.76	0.86	3.14	11.3	13.9	14.6	64	129	108	118	152	71
4.0	2.45	3.05	1.18	12.3	9.5	8.6	43	58	30	43	114	95
6.0	1.39	2.46	3.50	7.3	26	22	178	19	63	19	63	87
8.0	1.19	4.03	1.27	8.9	14	10.6	25	100	106	177	132	35
10.0	2.59	1.26	4.61	15	11.3	9.5	76	42	82	31	49	97.5
Avg	1.88	2.33	2.74	11.0	14.9	13.1	77	70	78	78	102	77
AVG		2.32			13.0			75			86	

functional groups where the OH functionality in the model system is attached to a long alkyl (C17) chain as opposed to a polyglucan chain in cellulose.

3.3. Roughness effect on force measurements

It has been shown that roughness plays an important role in force values obtained from atomic force microscopy (McKendry, Theoclitou, Abell & Rayment, 1998; Méndez-Vilas, González-Martín, Labajos-Broncano & Nuevo, 2002; Stifter, Weilandt, Marti & Hild, 1998) as surface forces, such as friction and adhesion are proportional to the surface contact area. To assess the effect of roughness on force interactions, we used cellulose films as model surfaces because of their low roughness and chemical composition homogeneity when compared to the bleached softwood kraft fibers. Roughness measurements with the AFM were made after a sample and tip had been equilibrated for 3 h in the solution. The roughness values for the various surfaces investigated are shown in Table 2. As expected, the fibers had much larger roughness and more variability than the film or SAM surfaces. The average RMS roughness value for the non-extracted and extracted fibers, ≈80 nm, are consistent with the upper limit of previously reported data for cellulosic fibers from wood and cotton (Juhue, Gayon, Corpart, Quet, Delichere, Charret, David, Cavaille & Perriat 2002; Snell, Groom & Rials, 2001).

Examining Figs. 4–6 and the data for surface roughness in Table 2, it appears that surface roughness does not seem to alter the magnitude of pull off forces significantly, as the average adhesion force values and the standard error of the measurement for the cellulose films, extracted fibers and non-extracted fibers are quite similar.

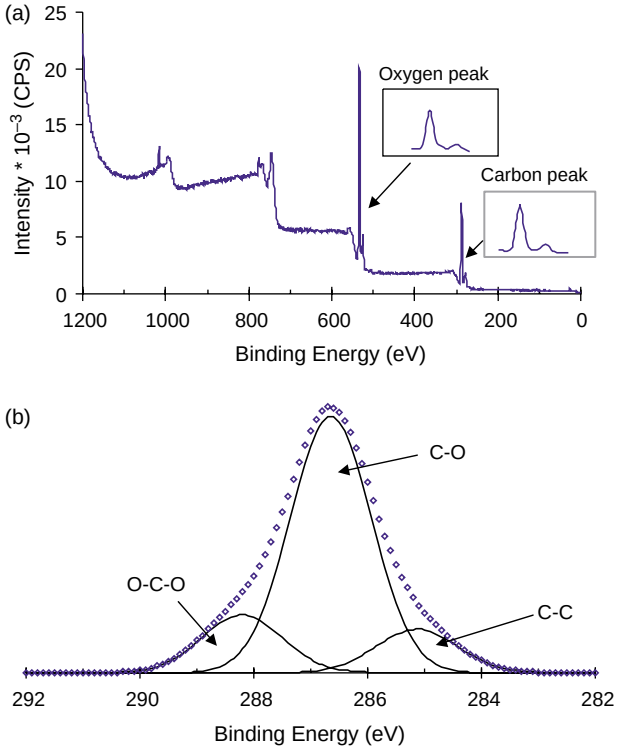

Fig. 7. XPS spectrum of extracted cellulose fiber: (a) survey spectra; (b) high resolution spectra of the resolved carbon 1s signal (included is the deconvolution spectra).

3.4. Surface composition and force measurements

X-ray photoelectron spectroscopy (XPS) and Fourier Transformed Infrared spectroscopy (FTIR), traditional techniques used in surface analysis, were employed to complement the AFM data. A representative low resolution survey spectrum and a corresponding high resolution spectrum of the carbon C 1s region from the extracted fiber are shown in Fig. 7. XPS data are summarized in Table 3. In cellulosic materials, four categories of carbon bonds can be identified by XPS: C1 carbons bonded to other carbons or hydrogen (C–C, C–H), C2 carbons bonded to one oxygen atom (C–O), C3 carbons attached to two oxygen atoms or a carbonyl group (C=O, O–C–O) and C4 carbons from carboxyl groups (O–C=O) (Zauscher, 2000a; Johansson, 2002; Beamson & Briggs, 1992; Laine, Stenius, Carlsson, & Strom, 1994). The deconvolution process employed did not find any C4 type carbons, consistent with the CFM results obtained using OH and CH_3 terminated tips.

Table 3
XPS analysis of cellulose samples

Cellulose sample	Peak area (%) by carbon type		
	C1	C2	C3
Film	13.6	70.0	16.4
Cellulose fiber	12.7	71.1	16.2
Extracted cellulose fiber	14.1	71.2	14.6
Theoretical	0	83.0	17.0

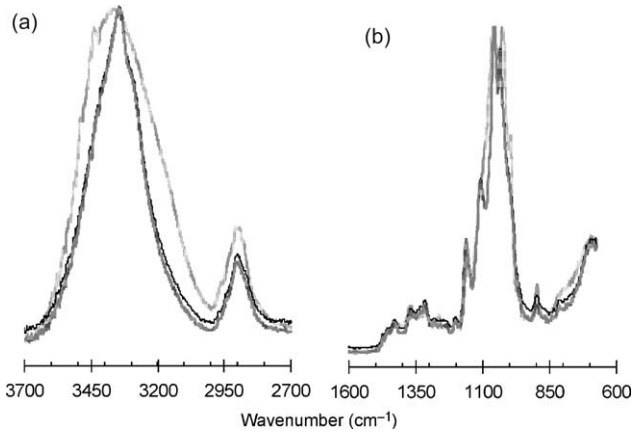

Fig. 8. ATR FTIR spectra of the cellulose samples (⋯⋯, cellulose film; ⋯⋯, cellulose fiber; —— extracted cellulose fiber): (a) 3700–2700 cm^{-1} region; (b) 1600–675 cm^{-1} region.

For pure cellulose, a large contribution of C2 (83%), and a small contribution of C3 (17%) carbons in the C(1s) peak is expected. However, a trimodal C(1s) peak with a small C1 component in addition to C2 and C3 contributions is universally observed (Holmberg, Berg, Stemme, Odberg, Rasmusson & Claesson 1997; Dorris & Gray, 1978; Hua, Situaru, Dennes & Young, 1997; Yamamoto & Ruddick, 1993; Zauscher, 2000b). XPS is a surface specific analysis technique that has a photoelectron escape depth (mean free path) of only a few nanometers, and the presence of the C1 contribution is therefore often associated with hydrocarbon contamination on the sample surface. Radiation damage of the cellulose surface has also been associated with the C1 contribution (Dorris & Gray, 1978). Alternatively, Hua et al. (Hua, Situaru, Dennes & Young 1997) suggest that part of the C1 peak intensity arises from C–C–O contributions (carbons 4 and 5 in the pyranose ring) that have a smaller binding energy than the hydroxylic carbon. These possibilities are supported by the observation that the ratio of the integrated intensities C3/(C1+C2) is usually in better agreement with the theoretical value of the C3/C2 ratio for cellulose than the C3/C2 ratio alone. This is also the case here, as can be seen from Table 3.

Increases in C1 component are normally employed as a method for surface extractives quantification (Laine, Stenius, Carlsson & Strom, 1994; Laine, Stenius, Carlsson & Strom, 1996). In this work, we find a small difference—1.4%—between the C1 area signals from extracted and non-extracted bleached softwood kraft samples (Table 3). However, we also found an intermediate value for the C1 area peak of the extracted cellulose film, between the values for extracted and non-extracted pulps. These results suggest that the amount of extractives on the sample surfaces is quite similar.

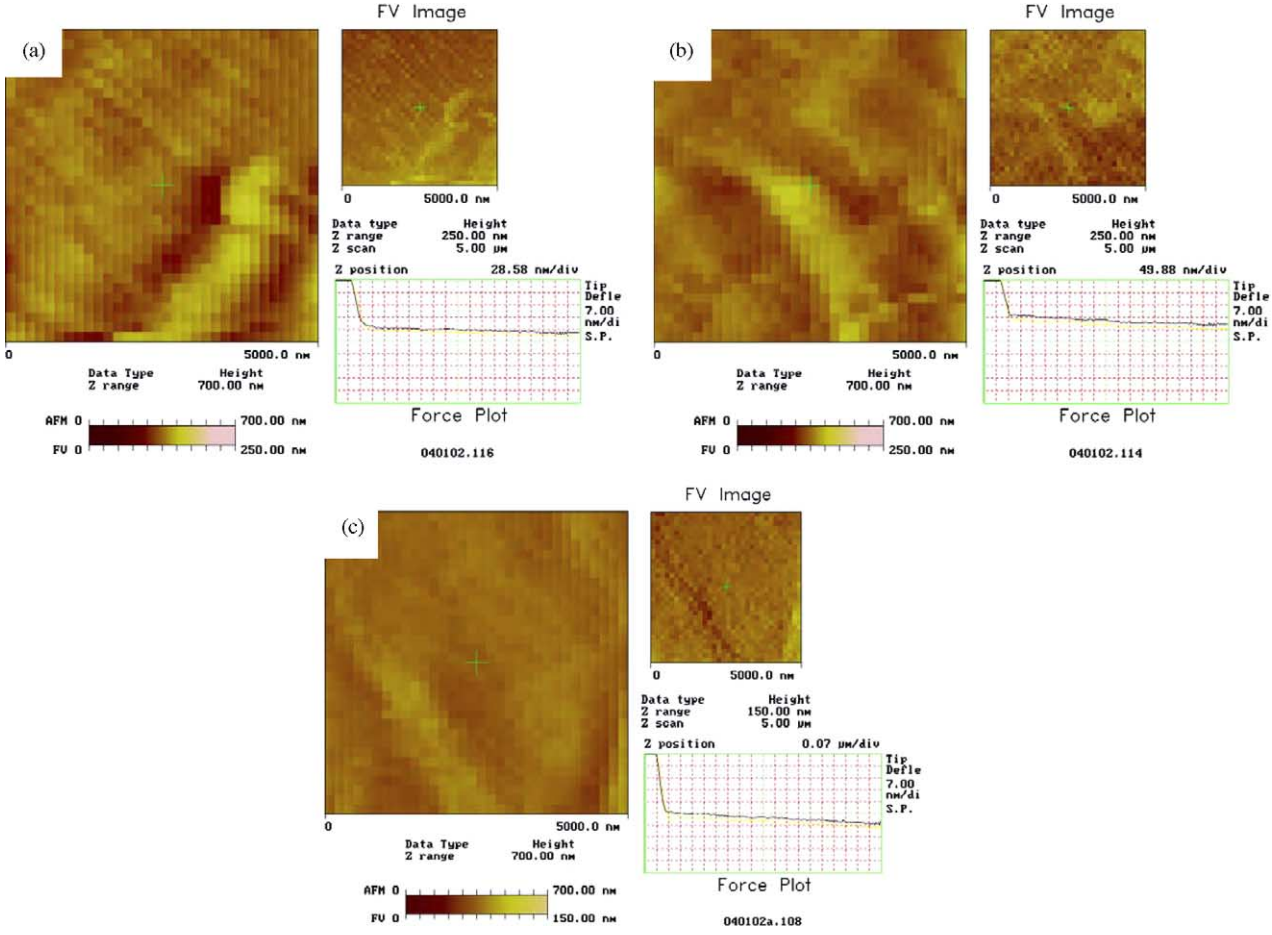

Fig. 9. Topographical and force mapping for the extracted cellulose fibers at different pH values using the OH terminated tip (a) pH=4.0; (b) pH=6.0; (c) pH=10.0.

Among the different FT-IR techniques for surface analysis, attenuated total reflectance (ATR) has the lowest depth penetration into the sample (sensitive up to 10 μm below the surface) (Forsskahl, Kentta, Kyyronen & Sundstrom, 1995). Two representative regions (3700–2700 cm^{-1} and 1600–675 cm^{-1}) of the ATR FT-IR spectra are shown in Fig. 8. The FT-IR spectra of the samples show no difference between extracted and non-extracted pulp samples, however, there are clear differences between the cellulose film and the pulp, cf Fig. 8. Those differences occur because regenerated cellulose films contain the cellulose II type structure, while pulp fibers (native cellulose) contain the cellulose I type. The cellulose II structure is able to form more hydrogen bonds than cellulose I, and this is reflected in a broader OH-stretching band in FTIR spectra for cellulose II, accompanied by a shift in the maximum frequency (Fig. 9(a)). The same type of broadening was found for the region 960–1500 cm^{-1}, where the bands assigned to vibrations of the pyranose ring and other bonds involving oxygen atoms are located (Ilharco, Garcia, da Silva & Ferreira, 1997). However, in the wavelength regions associated with extractive peaks, between 2800–2900 cm^{-1} for C–H stretching and 1700–1735 cm^{-1} for C=O stretching, no differences between the ATR-IR spectra of extracted and unextracted pulps or between the pulp fibers and the cellulose film were found. This is likely due to a limitation in the ATR technique (depth of analysis) and the location of extractives relative to the penetration depth of the technique (Kokkonen, Fardim & Holmbom, 2004).

Although XPS and FTIR are not true surface analytical techniques compared with CFM, and also are performed in different media, air for FTIR and vacuum for XPS, the information provided by them in our experiments support the force data obtained, in which a homogeneous surface composition in the studied samples can be suggested.

3.5. Force mapping of fiber surfaces

It is important to understand the local distribution of functional groups on the surface of the fibers, as it determines swelling behavior, chemical reactivity, etc. To gain an appreciation for the distribution of functional groups on the fiber surfaces, the pull-off forces were mapped and displayed graphically by force volume® imaging [Dimension 3000 Digital Instrument, Santa Barbara, California] at several pH values. Both the topographic image and the pull-off forces are shown in Figs. 9–11 for a square area of 5 μm by 5 μm at

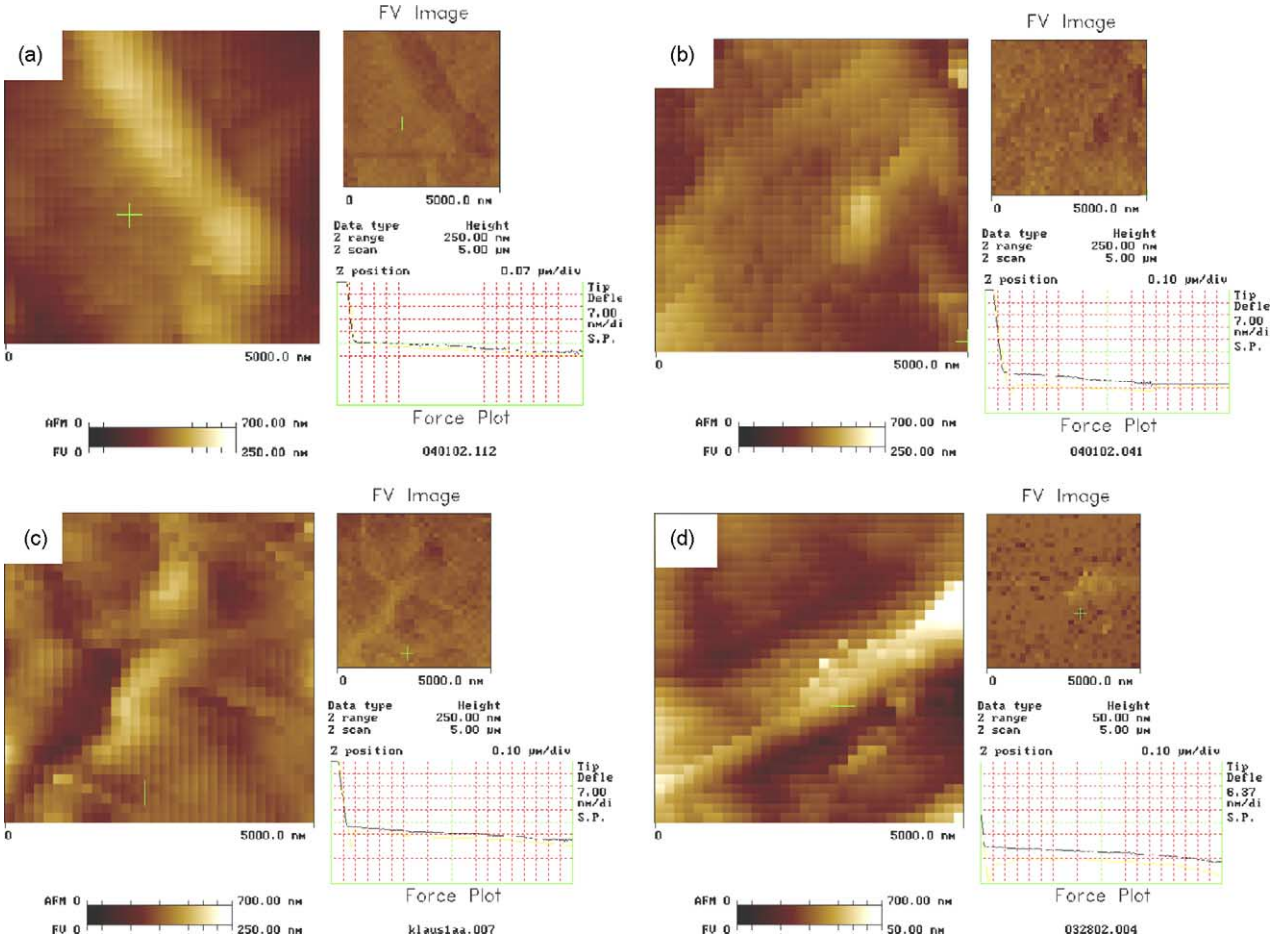

Fig. 10. Topographical and force mapping for the extracted cellulose fibers at different pH values using the COOH terminated tip (a) pH = 4.0; (b) pH = 6.0; (c) pH = 8.0; (d) pH = 10.0.

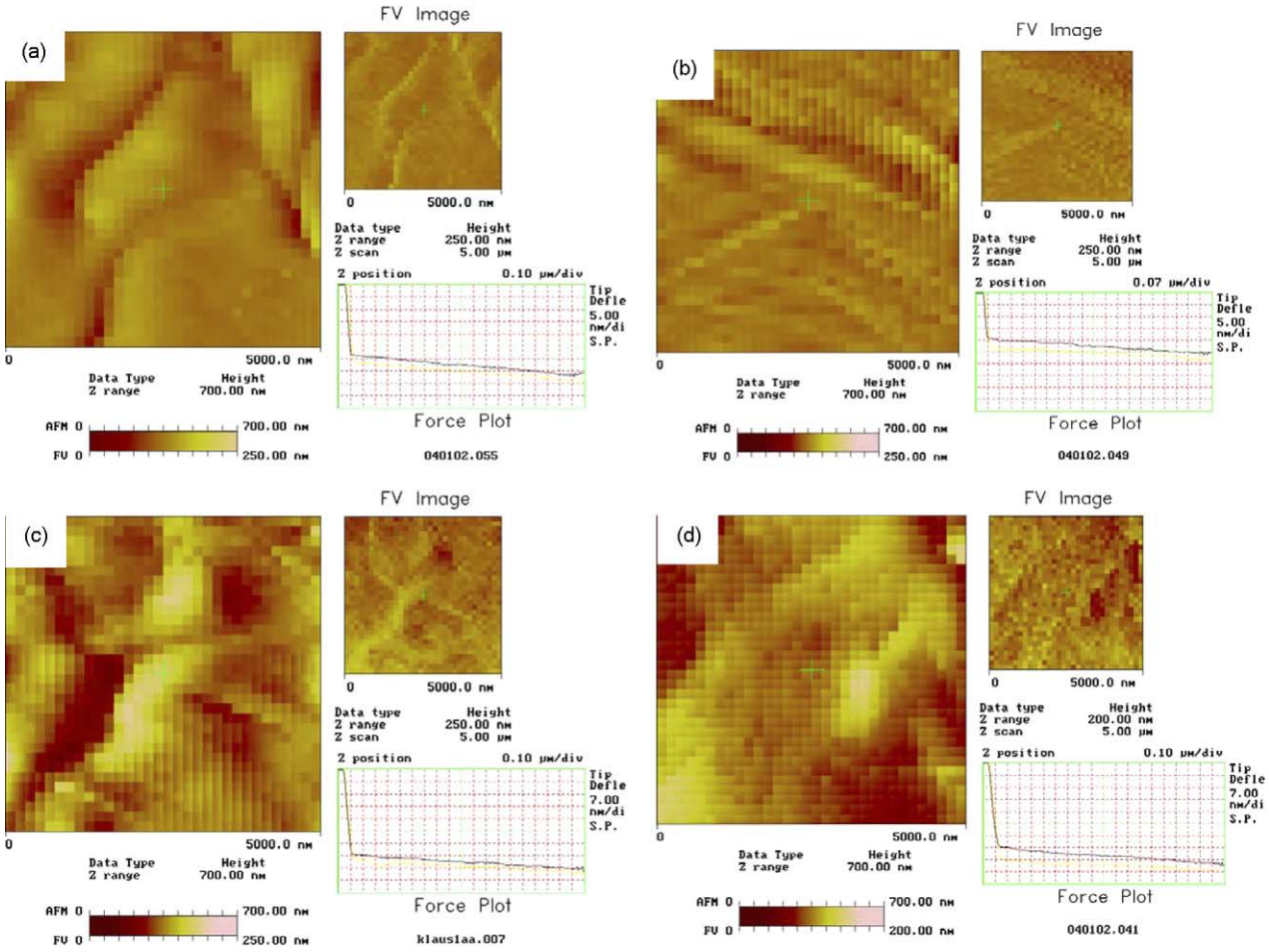

Fig. 11. Topographical and force mapping for the extracted cellulose fibers at different pH values using the CH CH3 terminated tip (a) pH=4.0; (b) pH=6.0; (c) pH=8.0; pH=10.0.

several pH values using modified tips. The force–volume (FV) images in Figs. 9–11 show that the chemical functionality of the pulp fiber surfaces is fairly uniform throughout and that topographically tall features are very slightly correlated with larger pull-off forces (adhesive interactions) at all pH values, irrespective of the solution pH. However, it is not possible to draw any conclusions about the effect of pH on the force interaction within an experimental set using a specific colloidal probe, because the image area at each pH value within a set differs, due to difficulties in finding the previously scanned area after changing the solvent.

4. Conclusions

Chemical force microscopy provides quantitative information on the interactions between chemically modified tips and the surface of self assembled monolayers, cellulose model surfaces, and bleached softwood Kraft pulp fibers. The magnitude of pull-off forces between modified tips and the fiber surface were comparable to results obtained from model cellulose surfaces. Using terminally functionalized SAM model surfaces we showed that CFM can distinguish between distinct chemical regions on a surface. Furthermore, CFM analysis of the regenerated cellulose film, cellulose fibers and extracted cellulose fibers show very similar surface chemistries, despite their large morphological differences. Force data, XPS and FT-IR analysis indicate that the cellulose film and commercial bleached softwood kraft fibers have relatively homogeneous surface chemical composition, despite the fibers having substantially higher RMS roughness values as compared to the film. Our results also suggest that regenerated cellulose membrane films are viable model surfaces that mimic the surface chemistry of much rougher natural cellulose fibers well.

Acknowledgements

The authors acknowledge North Carolina State University and Smurfit Carton de Colombia for support of this research.

References

Babcock, K. L., & Prater, C. B. (1995). *Phase imaging: Beyond topography* (pp. 1–4). Santa Barbara, CA: Digital Instruments.

Beamson, G., & Briggs, D. (1992). *High resolution XPS of organic polymers: The Scienta ESCA300 database*. Chichester, England: Wiley.

Boras, L., & Gatenholm, P. (1999). *Holzforschung*, *53*, 188–194.
Cappella, B., & Dietler, G. (1999). *Surface Science Reports*, *34*(1–3), 5–104.
Dorris, G. M., & Gray, D. G. (1978). *Cellulose Chemistry and Technology*, *12*, 9–23.
Duwez, A.-S., & Nysten, B. (2001). *Langmuir*, *17*, 8287–8292.
Duwez, A.-S., Poleunis, C., Bertrand, P., & Nysten, B. (2001). *Langmuir*, *17*, 6351–6357.
Forsskahl, I., Kentta, E., Kyyronen, P., & Sundstrom, O. (1995). *Applied Spectroscopy*, *49*(2), 163–170.
Freitas, A. M., & Sharma, M. M. (2001). *Journal of Colloid and Interface Science*, *233*(1), 73–82.
Furuta, T., & Gray, D. G. (1998). *Journal of Pulp and Paper Science*, *24*(10), 320–324.
Gray, D. G., Furuta, T., Pang, T., & Nilsson, B. (1991). In 11th international symposium on wood and pulping chemistry of conference, Nice.
Hanley, S. J., & Gray, D. G. (1995). In T. E. Conners, & S. Banerjee (Eds.), *Surface analysis of paper* (pp. 301–324). Boca Raton, FL: CRC Press.
He, H.-X., Huang, W., Zhang, H., Li, Q. G., Li, S. F. Y., & Liu, Z. F. (2000). *Langmuir*, *16*(2), 517–521.
Holmberg, M., Berg, J. C., Stemme, S., Odberg, L., Rasmusson, J., & Claesson, P. (1997). *Journal of Colloid and Interface Science*, *186*, 369–381.
Hua, Z. Q., Situaru, R., Dennes, F., & Young, A. (1997). *Plasmas and Polymers*, *2*(3), 199–224.
Ilharco, L. M., Garcia, A. R., da Silva, J. L., & Ferreira, L. F. V. (1997). *Langmuir*, *13*(15), 4126–4132.
Irvine, J., Aston, E., & Berg, J. C. (1999). *Tappi Journal*, *82*(5), 172–174.
Johansson, L.-S., Campbell, J. M., Koljonen, K., & Stenius, P. (1999). *Applied Surface Science*, *144–145*, 92–95.
Johansson, L.-S. (2002). *Microchimica Acta*, *138*(3–4), 217–223.
Juhue, D., Gayon, A. C., Corpart, J. M., Quet, C., Delichere, P., Charret, N., et al. (2002). *Textile Research Journal*, *72*(9), 832–843.
Kokkonen, P., Fardim, P., & Holmbom, B. (2004). *Nordic Pulp and Paper Research Journal*, *19*(3), 318–324.
Laine, J., Stenius, P., Carlsson, G., & Strom, G. (1994). *Cellulose*, 145–160.
Laine, J., Stenius, P., Carlsson, G., & Strom, G. (1996). *Paper Research Journal*, *11*(3), 201–210.
Méndez-Vilas, A., González-Martín, M. L., Labajos-Broncano, L., & Nuevo, M. J. (2002). *Journal of Adhesion Science and Technology*, *16*(13), 1737–1747.
Mansfield, S., De Jong, E., & Saddler, J. (1997). *Applied and Environmental Microbiology*, *63*(10), 3804–3809.
McKendry, R., Theoclitou, M.-E., Abell, C., & Rayment, T. (1998). *Langmuir*, *14*, 2846–2849.
Noy, A., Vezenov, D. V., & Lieber, C. M. (1997). *Annual Review of Materials Science*, *27*, 381–421.
Pang, L., & Gray, D. G. (1998). *Journal of Pulp and Paper Science*, *24*(11), 369–372.
Papastavrou, G., & Akari, S. (2000). *Colloids and Surfaces A: Physicochemical and Engineering Aspects*, *164*(2–3), 175–181.
Pereira, D. E. D., Chernoff, D., Claudio-Da-Silva, E. J., & Demuner, B. J. (2001). *ATIP*, *56*(2).
Prater, C. B., Maivald, P. G., Kjoller, K. J., Heaton, M. G. (1998). *Probing nanoscale forces with the atomic force microscopy* (pp. 16). Santa Barbara, CA: Digital Instruments.
Ron, H., & Rubinstein, I. (1994). *Langmuir*, *10*, 4566–4573.
Schönherr, H., Hruska, Z., & Vancso, J. (2000). *Macromolecules*, *33*, 4532–4537.
Schonherr, H., Hruska, Z., & Vancso, J. (1998). *Macromolecules*, *31*, 3679–3685.
Senden, T. J. (2001). *Current Opinion in Colloid and Interface Science*, *6*, 95–101.
Simola-Gustafsson, J., Hortling, B., & Peltonen, J. (2001). *Colloid and Polymer Science*, *279*(3), 221–231.
Sinniah, S. K., Steel, A. B., Miller, C. J., & Reutt-Robey, J. E. (1996). *Journal of the American Chemical Society*, *118*(37), 8925–8931.
Smith, D. A., Wallwork, M. L., Zhang, J., Kirkham, J., Robinson, C., Marsh, A., et al. (2000). *Journal of Physical Chemistry B*, *104*(37), 8862–8870.
Snell, R., Groom, L. H., & Rials, T. G. (2001). *Holzforschung*, *55*(5), 511–520.
Stifter, T., Weilandt, E., Marti, O., & Hild, S. (1998). *Applied Physics A Materials Science and Processing*, *66*(7), S597–S605.
Ton-That, C., Teare, D. O. H., & Bradley, R. H. (2000). *Chemistry of Materials*, *12*, 2106–2111.
Vezenov, D. V., Zhuk, A. V., Whitesides, G. M., & Lieber, C. M. (2002). *Journal of the American Chemical Society*, *124*(35), 10578–10588.
Wistara, N., Zhang, X., & Young, R. A. (1999). *Cellulose*, *6*, 325–348.
Yamamoto, K., & Ruddick, J. N. R. (1993). *Wood Protection*, *2*(2), 75–82.
Yokoyama, T., Kadla, J. F., & Chang, H.-M. (2002). *Journal of Agricultural and Food Chemistry*, *50*(5), 1040–1044.
Zauscher, S., & Klingenberg, D. J. (2001). *Colloids and Surfaces A: Physicochemical and Engineering Aspects*, *178*(1–3), 213–229.
Zauscher, S. (2000). *Polymer mediate surface interactions in pulp fiber suspension rheology. In Material Science* (pp. 409). Madison, Wisconsin: University of Wisconsin.
Zauscher, S. (2000). Polymer mediated surface interactions in pulp–fiber suspensions. PhD thesis, University of Wisconsin-Madison: Madison, WI.